

An Innovative Software for Stability Analysis of Multi-Energy Grids

Oriol Cartiel¹, Luis Sainz¹, and Juan José Mesas¹

¹ Department of Electrical Engineering (DEE)
Escola Tècnica Superior d'Enginyeria Industrial de Barcelona (ETSEIB)
Universitat Politècnica de Catalunya - BarcelonaTech (UPC)
Av. Diagonal 647, 08028 Barcelona, Spain.

Abstract. To effectively deal with the urgent climate crisis, clean resources and energy efficiency are becoming essential. As a result, renewable energy technologies (e.g., solar PV and wind power), HVDC links, and multi-energy systems have been widely integrated into traditional electrical power systems in recent decades. These technologies and HVDC links provide numerous benefits in driving the energy transition, and multi-energy systems are a promising energy storage/management solution to handle the variable and unpredictable nature of renewable energy technologies. However, despite the many benefits of the above new sustainable energy infrastructures, they also pose new technological challenges, such as small-signal stability problems due to poorly damped resonances caused by the interaction between power electronics and traditional grid elements. Current tools are not fully effective in studying these issues yet. Given this scenario, this paper presents an *Innovative Software for Stability Analysis*, a novel tool designed for small-signal stability assessment in multi-energy grids. This *software* enables accurate stability predictions and provides actionable solutions to mitigate instabilities, regardless of system size. Its capabilities are demonstrated through comprehensive MATLAB/Simulink simulations on various systems, including a IEEE 3-bus test system, an AC/DC multi-energy grid with hydrogen vector, and a 70k-bus synthetic test system.

Keywords. Damping solutions, multi-energy grids, positive-mode-damping, resonance mode analysis, stability assessment.

1. Introduction

The increase in worldwide greenhouse gas emissions and the high price of fossil fuels have accelerated the global transition towards eco-friendly energy technologies [1]. To reduce environmental pollution and address the climate emergency, the traditional concept of the Electric Power System (EPS) must evolve into a more sustainable paradigm. In this transformation, Renewable Energy Technologies (RETs) must prevail over others, as they offer clean alternatives that enhance energy efficiency and reduce dependency on hydrocarbons.

In this context, Multi-Energy Grids (MEGs) have gained significant attention [2]. MEGs integrate multiple energy vectors (e.g., electricity, hydrogen, natural gas, and thermal energy), enabling higher efficiency compared to

single-source systems. Their inherent resource complementarity allows for seamless integration of RETs, reduced energy costs, and enhanced reliability. For instance, green hydrogen can be produced using RETs within MEGs, stored for later use, and applied in transportation or grid support via fuel cells [3]. Furthermore, MEGs facilitate the adoption of Energy Storage Systems (ESSs) and novel energy conversion processes, such as power-to-gas and gas-to-power technologies, fostering resilience and operational flexibility [4]. However, alongside these benefits, the proliferation of power electronics in RETs, ESSs, and energy conversion units creates complex interactions that can compromise stability, often manifesting as oscillatory phenomena from interactions between the transmission grid, converter controls, and energy vectors, potentially resulting in poorly damped resonances [5], [6], [7], [8].

Traditional methods and tools are insufficient to address these problems in MEGs. On one hand, resonances are traditionally identified through frequency scan analysis, limited in scope as it identifies resonance frequencies without offering actionable solutions [9]. Resonance Mode Analysis (RMA) improves by providing detailed insights into grid component contributions to resonances and the best locations to damp them [10]. However, RMA's computational complexity makes it impractical for large-scale systems, such as MEGs with many buses [11], [12]. An alternative RMA-based methodology in the literature reduces this computational effort and time [12]. On the other hand, the transformation of EPSs necessitates up-to-date methods for dynamic stability assessment. In systems dominated by power electronics, oscillatory phenomena are classified as small-signal *converter-driven stability* [6], characterised by fast-dynamic interactions (typically tens to hundreds of Hz, and potentially up to kHz) caused by small disturbances. These phenomena are best studied through linearised models around the system's operating point, using approaches classified into time-domain eigenvalue analysis and impedance-based frequency-

domain methods [5], [13], [14], [15].

Time-domain eigenvalue techniques are widely used state-space tools that provide a complete overview of system dynamics and allow the influence of grid and power electronics control parameters on stability to be assessed using Participation Factors (PFs) [5]. Nevertheless, stability of multi-terminal power electronics-based systems with energy vector integration is difficult to analyse, as detailed information about all elements of the system (not provided by manufacturer black-box models) and high-order dynamic models are required [16]. Frequency-domain methods have become established in the last decade as an alternative tool for assessing stability with less computational effort and detailed system information (e.g., black-box models can be used). While early approaches, such as the Nyquist, Bode, and positive-net-damping criteria, focused on local stability in single-input single-output systems [13], more recent methods extend these principles to multi-terminal grids, accommodating multiple-input multiple-output dynamics [15], [17]. Among these advanced methodologies, the Generalised Nyquist Criterion (GNC) and the Positive-Mode-Damping (PMD) stability criterion have emerged as promising tools for frequency-domain analysis [15], [17]. GNC evaluates system stability using eigenvalues of the open-loop transfer function but is hindered by limitations such as dependency on subsystem partitioning and lack of intuitive results analysis [15], [16], [17]. Conversely, the PMD stability criterion has been proposed to address GNC's drawbacks [15], offering a practical and intuitive method based on RMA [10], [11], enabling practical stability assessment and offering insights into resonance damping solutions [15], [18], [19].

Building on these developments, this paper introduces an *Innovative Software for Stability Analysis*, a novel tool designed to enhance small-signal *converter-driven stability* studies in MEGs. This software

- Overcomes computational challenges of existing methods while maintaining accuracy.
- Simplifies stability assessment with a user-friendly interface.
- Integrates black-box models, enabling analysis without detailed system (i.e., white-box) models.

- Uses PF-based sensitivity analyses to identify critical grid components and their impact.
- Provides a quantitative stability measure using a Damping Margin (DM) indicator [19].
- Facilitates the design of damping solutions.
- Supports the study of extremely large MEGs.

The above features make the *software* a robust tool for addressing stability concerns in multi-terminal systems dominated by power electronics. To demonstrate and evaluate the capabilities of the *software*, comprehensive studies are conducted using MATLAB/Simulink (MATSIM) simulations on three different systems: (i) the IEEE 3-bus test power system [20], (ii) an AC/DC MEG incorporating hydrogen vector, and (iii) the Eastern USA 70k-bus synthetic test power system [21].

2. Innovative Software for Stability Analysis

A high-performance software-based tool is presented for conducting small-signal *converter-driven stability* [6] studies of MEGs in a simple, efficient, and reliable manner using the PMD stability criterion, a frequency-domain approach. The *software* comprises five main blocks, leveraging n -bus MEG data provided by either white- or black-box models (see Fig. 1):

1. Nodal admittance matrix construction (Section 2.A).
2. RMA methodology application (Section 2.B).
3. PMD stability criterion assessment (Section 2.C).
4. Damping margin analysis (Section 2.D).
5. Damping compensator design (Section 2.E).

B. Nodal Admittance Matrix

Fig. 2 illustrates the schematic diagram of a multi-terminal transmission MEG comprising a transmission grid characterised by its nodal admittance matrix $\mathbf{Y}_G(s)$, external components connected to the grid buses (including power electronics-based converters), and energy vectors. The external components and energy vectors are represented by the equivalent admittance matrix $\mathbf{Y}_c(s) = \text{diag}(\mathbf{Y}_{c,1}(s) \dots \mathbf{Y}_{c,n}(s))$ and the bus current injection vector $\mathbf{I}_B(s) = [\mathbf{I}_{B,1}(s) \dots \mathbf{I}_{B,n}(s)]^T$, respectively. The relationship between the bus voltages and currents at the multi-terminal transmission MEG is

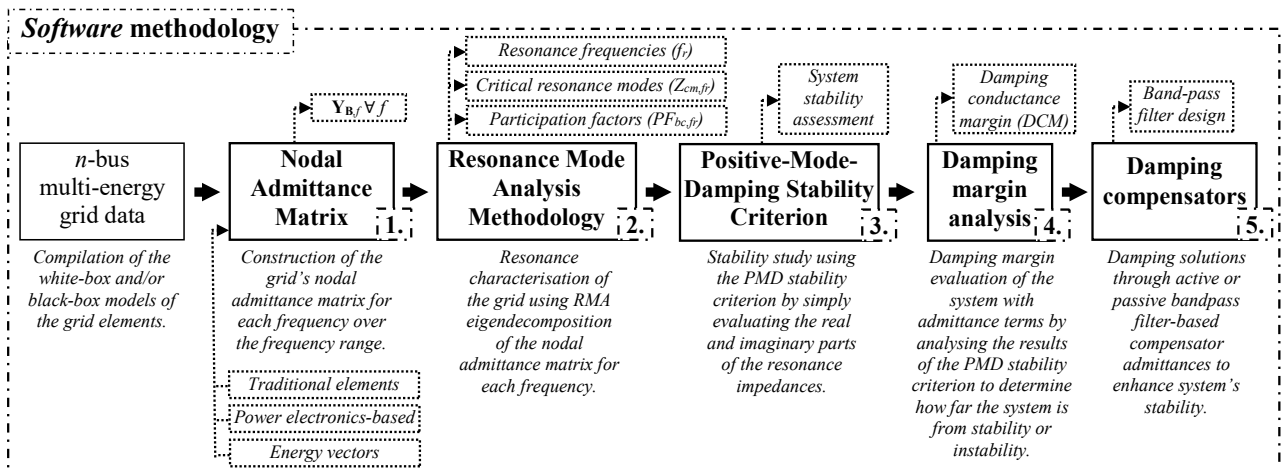


Fig. 1. Flowchart of the *software* methodology.

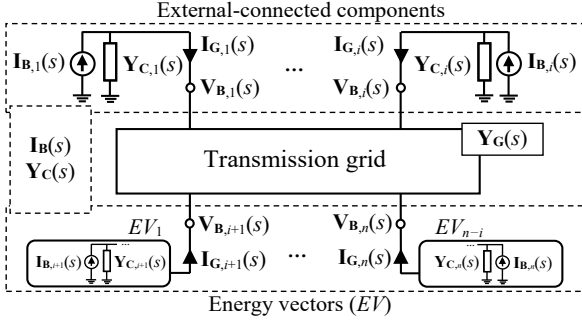


Fig. 2. Schematic diagram of a multi-terminal transmission MEG.

expressed using the voltage node method as follows:

$$\left. \begin{aligned} \mathbf{I}_G(s) &= \mathbf{Y}_G(s) \mathbf{V}_B(s) \\ \mathbf{I}_G(s) &= \mathbf{I}_B(s) - \mathbf{Y}_C(s) \mathbf{V}_B(s) \end{aligned} \right\} \Rightarrow \quad (1)$$

$$\mathbf{V}_B(s) = (\mathbf{I} + \mathbf{Z}_G(s) \mathbf{Y}_C(s))^{-1} \mathbf{Z}_G(s) \mathbf{I}_B(s) = \mathbf{Y}_B^{-1}(s) \mathbf{I}_B(s),$$

where \mathbf{I} is the identity matrix, $\mathbf{Z}_G(s) = \mathbf{Y}_G^{-1}(s)$ is the grid impedance matrix, $\mathbf{V}_B(s)$ is the bus voltage vector, and $\mathbf{Y}_B(s)$ is the nodal admittance matrix of the multi-terminal transmission MEG.

The nodal admittance matrix $\mathbf{Y}_B(s)$ is a square, symmetric (except in cases involving non-reciprocal branches), and non-Hermitian matrix. It characterises MEGs with n buses and establishes the relationship between the current injection vector $\mathbf{I}_B(s)$ and the nodal voltage vector $\mathbf{V}_B(s)$ at the respective buses (see (1)).

Modern transmission grids are characterised by their large-scale and sparse topologies, resulting in extensive yet sparse nodal admittance matrices [12]. These properties play a critical role in the functionality of the *software* tool, as the nodal admittance matrix is the foundational mathematical entity in grid characterisation. Its simplicity, versatility, and widespread acceptance within the scientific community make it invaluable for numerous applications. Thus, a key goal of the *software* tool is to incorporate all grid elements present in the MEG—ranging from traditional components to power electronics-based devices and energy vectors—into the nodal admittance matrix. This integration ensures accurate system modelling and facilitates the analysis of stability and resonance phenomena.

In many cases, detailed white-box models for specific grid components, such as power electronics-based devices, are unavailable. Instead, manufacturers typically provide their impedance or admittance frequency profiles as black-box models, which can also be obtained through direct measurements. In such scenarios, these black-box models can be integrated into the calculation of the nodal admittance matrix $\mathbf{Y}_B(s)$ (1) (see [12], [18] for details).

C. Resonance Mode Analysis Methodology

RMA is based on the eigenvalue decomposition of the nodal admittance matrix $\mathbf{Y}_B(s)$ over a frequency scan range [10]. For a given n -bus grid, the eigenvalue decomposition at a particular frequency f yields the modal voltage vector \mathbf{U}_f , the modal current vector \mathbf{J}_f , and the diagonal eigenvalue matrix $\mathbf{\Lambda}_{Y,f}$. The corresponding right \mathbf{R}_f and left

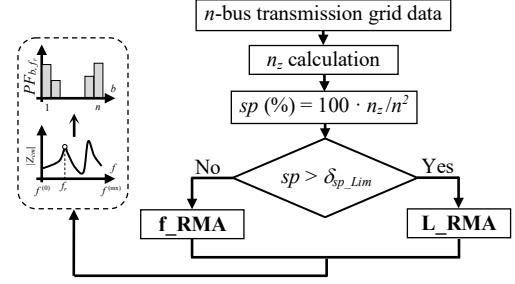


Fig. 3. Flowchart of RMA-based methodology.

$\mathbf{L}_f = \mathbf{R}_f^{-1}$ eigenvector matrices link these modes. I.e.,

$$\mathbf{V}_{B,f} = \mathbf{Y}_{B,f}^{-1}(s) \mathbf{I}_{B,f} \Rightarrow \mathbf{U}_f = \mathbf{\Lambda}_{Y,f}^{-1} \mathbf{J}_f$$

$$\mathbf{\Lambda}_{Y,f} = \begin{bmatrix} \lambda_{y1} & \cdots & 0 \\ \vdots & \ddots & \vdots \\ 0 & \cdots & \lambda_{yn} \end{bmatrix}_f = \mathbf{L}_f \mathbf{Y}_{B,f}(s) \mathbf{R}_f \begin{cases} \mathbf{U}_f = \mathbf{L}_f \mathbf{V}_{B,f} \\ \mathbf{J}_f = \mathbf{L}_f \mathbf{I}_{B,f} \end{cases} \quad (2)$$

At resonance frequencies f_r , singularities in $\mathbf{Y}_B(s)$ are characterised by critical eigenvalues of $\mathbf{\Lambda}_{Y,f}$, known as critical resonance modes Z_{cm,f_r} . These singularities manifest as peaks in the modal impedance magnitudes, $Z_{mj,f} = 1/\lambda_{yj,f}$, where $Z_{mj,f}$ represents the modal impedance of the j -th mode [10]. RMA also evaluates the excitability and observability of critical resonance modes at specific grid buses using PFs, defined as $PF_{bj} = R_{bj} \cdot L_{jb}$, where b is the bus index and j the mode number [10]. Thus, determining the largest modulus eigenvalue of the impedance matrix at each frequency is sufficient for resonance studies (i.e., the critical modes $Z_{cm,f}$) [11]. Accordingly, an RMA-based methodology is presented in [12], which only calculates the largest modulus eigenvalue of $\mathbf{Y}_{B,f}(s)$ and its corresponding right and left unit eigenvectors. Fig. 3 illustrates how this methodology incorporates two paths:

1. *Faster RMA (f_RMA)*: Suited for small grids.
2. *Lanczos-based RMA (L_RMA)*: Optimised for grids with large and sparse nodal admittance matrices.

The choice between f_RMA and L_RMA is determined by the sparsity ratio sp of $\mathbf{Y}_B(s)$. The sp of the $n \times n$ nodal admittance matrix $\mathbf{Y}_B(s)$ can be calculated as,

$$sp(\%) = 100 n_z / n^2, \quad (3)$$

where n_z is the total number of zero elements within $\mathbf{Y}_B(s)$. If $sp > \delta_{sp_lim}$ (with recommended δ_{sp_lim} limit [12]: 98%) L_RMA is used; otherwise, f_RMA is preferred. Both methodologies provide critical mode c curves ($|Z_{cm}|$) and PFs (PF_{bc}) across the frequency range, enabling effective resonance and stability analysis in MEGs. See [12] for further details on the methodology.

D. Positive-Mode-Damping Stability Criterion

The PMD stability criterion [15], [18] based on the RMA eigenvalue decomposition is used in the *software* for easy and practical stability assessment of multi-terminal MEGs in the frequency-domain. The grid's stability assessment is performed through the study of critical resonance modes Z_{cm,f_r} (largest modulus modal

impedance) at resonance frequencies f_r applying the following criterion: the grid is stable iff

$$\sigma_{f_r} \approx \frac{R_{cm,f_r}}{m_{x,f_r}} < 0 \quad (m_{x,f_r} = \partial X_{cm,f_r} / \partial f|_{f=f_r}) \quad \forall f_r, \quad (4)$$

where $-\sigma_{f_r}$ represents the damping of the system oscillatory mode at f_r , R_{cm,f_r} and X_{cm,f_r} are the real and imaginary parts of the critical resonance modes Z_{cm,f_r} , respectively, and m_{x,f_r} is the slope of X_{cm,f_r} .

E. Damping Margin Analysis

To determine the DM of the system, the margin associated with the impedance critical modes must be determined for each resonance frequency (local DM) [19]. This will yield the damping stability margins at the given resonance frequencies, either to stabilise the system or to enhance stability.

According to [19], the DM indicator, obtained from PMD stability criterion results, is:

$$DCM_{h,f_r} \approx \text{Re} \left\{ 1 / \left(PF_{hc,f_r} Z_{cm,f_r} \right) \right\}, \quad (5)$$

where DCM_{h,f_r} corresponds with the damping conductance margin at f_r and PF_{hc,f_r} is the PF of the most affected bus b by the critical mode Z_{cm,f_r} ($b = h$ and $j = c$).

All local DMs are required to assess the system's stability degree through a global DM, DCM , of the system. Two definitions for this global DM are possible: i) given an unstable system, the global DM is defined by the greatest absolute value of the local DMs characterising instability; ii) given a stable system, the global DM is defined by the smallest value of the local DMs of the system. See [19] for further details on the DM indicator.

F. Damping Compensators

Different approaches exist to mitigate resonance instabilities, and this tool proposes two possible methods: active and passive damping compensators. According to Section 2.D and [19], the aim is to improve all the local DM that characterise instability by adding a compensation admittance $Y_{cp}(s)$ at bus h . This admittance should satisfy the condition $|G_{cp,f_r}| \geq |DM_{h,f_r}|$ and be of opposite sign [19], where G_{cp,f_r} is the real part of $Y_{cp}(s)$ at f_r .

The modelling of both compensators is based on a bandpass filter-based compensation admittance, with a gain equal to G_{cp,f_r} and a centre frequency at f_r . Fig. 4 illustrates the characteristic curve of the compensator admittance transfer function, which is defined as:

$$Y_{cp}(s) = \frac{\omega_r \frac{G_{cp,f_r}}{Q} s}{s^2 + \frac{\omega_r}{Q} s + \omega_r^2} \quad (\omega_r = 2\pi f_r), \quad (6)$$

where Q is a Q-factor (reciprocal of the filter bandwidth) whose value depends on the stability issue [19]. According to Fig. 4, by matching the frequency to be compensated with the resonance frequency of the compensator, the necessary damping is added to the system to stabilise it.

Active damping compensator is addressed by modifying

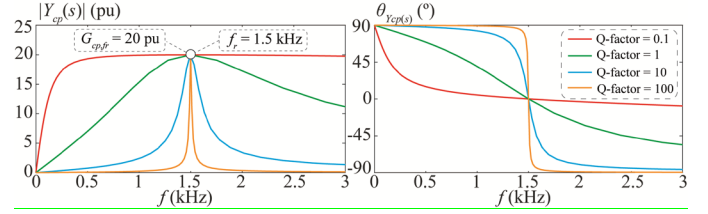


Fig. 4. Bandpass filter-based frequency response.

the equivalent admittance of the VSC with a feed-forward filter in the current control loop, while passive damping compensator by connecting a compensation admittance of a shunt $R_{cp} - L_{cp} - C_{cp}$ filter to the bus terminals [19].

3. Computational Techniques

The *software* can be developed in any programming environment; however, in this work, it is implemented in MATLAB due to its extensive library of functions and toolboxes, including sparse matrix techniques and the Parallel Computing Toolbox, which significantly enhance computational efficiency. Transmission grids often produce sparse nodal admittance matrices, as the limited node-to-node connections result in many zero elements. This sparsity increases with grid size, making dense matrix representations inefficient due to high memory requirements to store surplus zeros. By adopting sparse matrix techniques, the *software* optimises memory usage and accelerates calculations in large-scale systems. Additionally, parallel computation, enabled by MATLAB's Parallel Computing Toolbox, leverages multi-core processors to efficiently handle data-intensive tasks. This approach significantly reduces computation time for repetitive operations such as RMA calculations across wide frequency ranges, ensuring the *software* is both efficient and scalable.

4. Application and Tests

This section evaluates the *software* through three case studies: a small grid, where the results are compared with MATSIM time-domain simulations to verify correctness, and two additional grids—a MEG with hydrogen vector as black-box models and a 70k-bus supergrid—demonstrating its scalability, suitability, and computational efficiency for complex scenarios, impractical for MATSIM approaches.

A. Comparison of the Software vs. MATLAB/Simulink

The modified IEEE 3-bus test power system, which includes an additional fourth bus connected to bus 2 via a transformer (see Fig. 2(a) in [19]) is studied. A VSC with parameters from [11] and a shunt capacitor are connected to this fourth bus [19]. The *software* is applied to an unstable case of this system, with results summarised in Fig. 5(a). A critical resonance mode at 1.25 kHz is detected using the PMD stability criterion (4), with $R_{cm,1.25} \cdot m_{x,1.25} > 0$. The highest PF is $PF_{4c,1.25}$, indicating bus 4 as the most affected node. The local DM for this mode is $DCM_{4,1.25} \approx -0.0163$ pu, whose absolute value

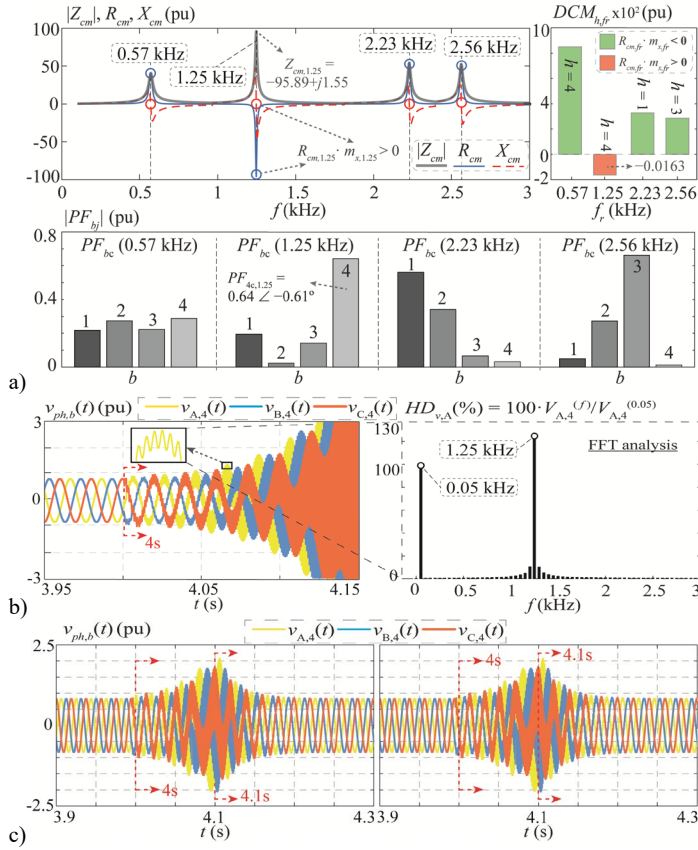


Fig. 5. IEEE 3-bus power system [20] stability assessment: a) PMD stability criterion and DCM analysis results. b) Time-domain simulation of bus 4 voltage. c) Time-domain simulations of bus 4 voltage with active (left) and passive (right) compensator.

matches the global DM, $DCM = |DCM_{4,1.25}|$, because is the only local DM characterising system instability. MATSIM time-domain simulations verify the instability, showing voltage oscillations at 1.25 kHz at bus 4 after the VSC connection at 4 s (see Fig. 5(b)). Active and passive damping compensators, designed using the fifth step of the *software* in Fig. 1, ensure stability as the critical resonance mode at 1.25 kHz satisfies the stability criterion (4) (results not shown for brevity). The design values, with $Q = 10$, are (see Section 2.E): i) Active compensator: $G_{cp,fr} = 0.0326$ pu; ii) Passive compensator: $R_{cp} = 30$ pu, $L_{cp} = 3.83 \times 10^{-2}$ pu, and $C_{cp} = 4.25 \times 10^{-7}$ pu. Simulations in Fig. 5(c) confirm that voltage stabilises at 4.1 s after compensator connection, thanks to their damping effect.

Additionally, the following aspects highlight the differences in efficiency and practicality between the *software* and MATSIM:

- **Execution Time:** The *software* analyses stability in 0.47 s, while MATSIM requires approx. 28 s due to the time-domain simulation overhead.
- **Ease of Setup:** The *software* uses simple input data, while MATSIM requires full manual circuit construction, becoming impractical for larger grids.
- **Scalability:** The *software* is scalable to large grids due to its reliance on the nodal admittance matrix, whereas MATSIM simulations are limited by computational resources as grid size increases.
- **Black-Box Models:** The *software* can integrate black-box impedance/admittance profiles directly.

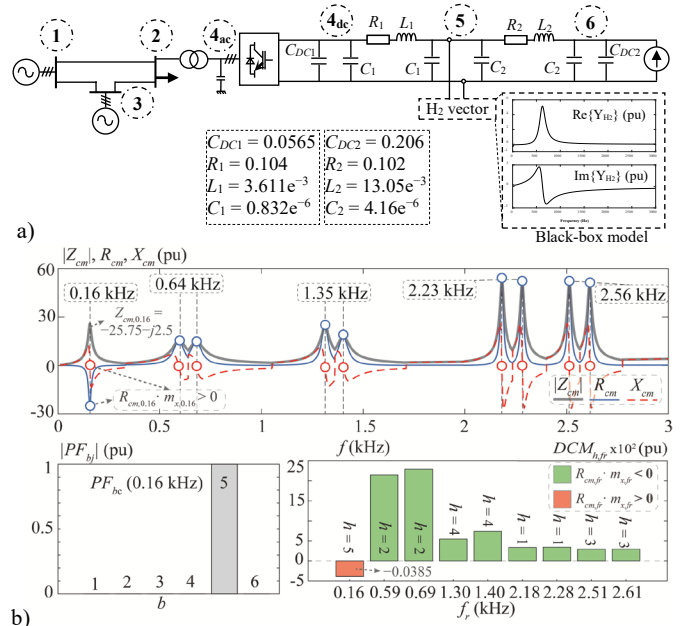


Fig. 6. MEG stability assessment: a) An AC/DC IEEE 3-bus power system-based [20] MEG with hydrogen vector connected (all values in per-unit). b) PMD stability criterion and DCM analysis results.

B. Stability Tests with the Software

The computational efficiency of the *software* is evaluated in two additional cases that are impractical for MATSIM time-domain simulations due to the inclusion of black-box models and the large grid size.

1) Test #1 – AC/DC Multi-Energy Grid with Hydrogen Vector

Fig. 6(a) illustrates an AC/DC IEEE 3-bus power system-based MEG incorporating hydrogen vector. The AC/DC link uses the dq -complex three-port VSC analytical model from [14], while the hydrogen vector is studied using their black-box model. The *software* is applied to an unstable case of this system, with results summarised in Fig. 6(b). A critical resonance mode at 0.16 kHz is identified using the PMD stability criterion (4), with $R_{cm,0.16} \cdot m_{x,0.16} > 0$. The highest PF is $PF_{5c,0.16}$, indicating bus 5 as the only affected node. This confirms that the resonance is only caused by the hydrogen vector connected to bus 5 at the DC side. The local DM for this mode is $DCM_{5,0.16} \approx -0.0385$ pu, whose absolute value matches the global DM, $DCM = |DCM_{5,0.16}|$, as it is the only local DM characterising instability. Since no VSCs are connected to bus 5, only a passive damping compensator can be designed to ensure stability. The design values are: $Q = 1$, $R_{cp} = 12$ pu, $L_{cp} = 1.12 \times 10^{-2}$ pu, and $C_{cp} = 9.27 \times 10^{-5}$ pu. This compensator allows to satisfy the stability criterion (4) for the critical resonance mode at 0.16 kHz (results not shown for brevity).

2) Test #2 – Multi-Terminal HVDC Hybrid AC/DC Supergrid

Fig. 7(a) depicts the modified Eastern USA 70k-bus synthetic test power system [21], a supergrid test case. It includes seven additional VSC-connected systems (with

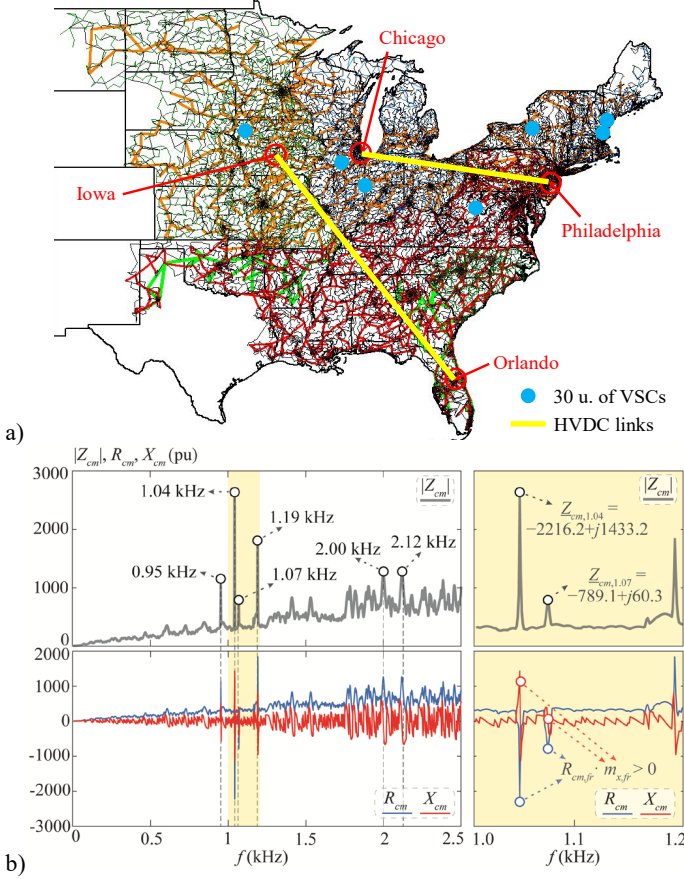


Fig. 7. Multi-terminal HVDC hybrid AC/DC supergrid stability assessment: a) Modified Eastern USA 70k-bus synthetic test power system [21]. b) PMD stability criterion and DCM analysis results.

30 units of 690 V 1 MVA VSCs) at buses 1, 804, 805, 11904, 18247, 34601, and 43907, with parameters from [11]. Two HVDC links (440 kVdc, 500 MW) using the three-port VSC analytical model from [14] connect Philadelphia (bus 13337) with Chicago (bus 43323) (~1200 km) and Iowa (bus 54262) with Orlando (bus 62453) (~2300 km). The *software* is applied to an unstable case, with results summarised in Fig. 7(b). Two critical resonance modes at 1.04 kHz and 1.07 kHz fail to meet the PMD stability criterion (4), as $R_{cm,fr} \cdot m_{x,fr} > 0$ for both. The highest PFs are $PF_{18247,1.04} = 0.1238 \text{ pu} \angle 0^\circ$ and $PF_{1,1.07} = 0.0844 \text{ pu} \angle 0^\circ$, indicating that buses 18247 and 1 as having the most significant participation in the respective resonances. The local DMs for these modes are $DCM_{18247,1.04} \approx -0.0029 \text{ pu}$ and $DCM_{1,1.07} \approx -0.0148 \text{ pu}$. The absolute value of $DCM_{1,1.07}$ matches the global DM, $DCM = |DCM_{1,1.07}|$, as it is the largest absolute value among the local DMs characterising instability. Active damping compensators are designed for buses 18247 and 1 to stabilise both resonances, with $Q = 10$, and $G_{cp,fr} = 0.01 \text{ pu}$ and 0.03 pu , respectively. These compensators ensure stability by satisfying the PMD stability criterion (4) for the modes at 1.04 kHz and 1.07 kHz (results not shown for brevity). Finally, the computational efficiency of the *software* is noteworthy, solving the 70k-bus supergrid in approximately 9 minutes (~553 s). By comparison, other methods could require tens of hours or even days [12].

5. Conclusion

This paper introduces an *Innovative Software for Stability Analysis*, a novel tool designed for small-signal stability assessment in MEGs. By addressing the limitations of existing methods, the *software* supports accurate stability evaluation across systems of varying complexity and scale (i.e., from small to large grids). Its features include computational efficiency, a user-friendly operation, and the ability to integrate black-box models (thus avoiding detailed internal system representations). Furthermore, the *software* incorporates advanced functionalities such as PF-based sensitivity analysis and the DM indicator to identify the most influential buses on critical resonance modes, assess how far the system is from stability/instability, and propose effective damping solutions. The *software's* capabilities were demonstrated through comprehensive MATSIM simulations across three distinct case studies: an IEEE 3-bus power system, an AC/DC MEG with an integrated hydrogen vector, and a 70k-bus synthetic test system. These studies showcase its efficiency in handling exceedingly complex systems and highlight its potential as a benchmark tool for stability analysis in MEGs. Future research will focus on extending the *software* to support real-time interaction with Hardware-In-the-Loop (HIL) platforms, enabling direct interfacing for stability analysis. While it can already integrate black-box models extracted from HIL systems, real-time interconnection between both environments is not yet supported.

Acknowledgement

This work was supported by Ministerio de Ciencia, Innovación y Universidades, Agencia Estatal de Investigación, FEDER, UE (Grant PID2021-123633OB-C33 supported by MICIU/AEI/10.13039/501100011033 / FEDER, UE).

References

- [1] "Horizon Europe | European Commission." Accessed: Jan. 23, 2025. [Online]. Available: [Horizon Europe Website](https://ec.europa.eu/horizon-europe/).
- [2] E. Guelpa, A. Bisch, V. Verda, M. Chertkov, and H. Lund, "Towards future infrastructures for sustainable multi-energy systems: A review," in *Energy*, vol. 184, pp. 2–21, Oct. 2019.
- [3] C. Yang, "Hydrogen and electricity: Parallels, interactions, and convergence" in *International Journal of Hydrogen Energy*, vol. 33, no. 8, pp. 1977–1994, April 2008.
- [4] J. Li, G. Li, S. Ma, Z. Liang, Y. Li, and W. Zeng, "Modeling and Simulation of Hydrogen Energy Storage System for Power-to-gas and Gas-to-power Systems," in *Journal of Modern Power Systems and Clean Energy*, vol. 11, no. 3, pp. 885–895, May 2023.
- [5] P. Kundur, "Power system stability and control," McGraw-Hill, 1994.
- [6] N. Hatziaargyriou *et al.*, "Definition and Classification of Power System Stability – Revisited & Extended," in *IEEE Transactions on Power Systems*, vol. 36, no. 4, pp. 3271–3281, July 2021.
- [7] J. Sun *et al.*, "Renewable energy transmission by HVDC across the continent: system challenges and opportunities,"

- in *CSEE Journal of Power and Energy Systems*, vol. 3, no. 4, pp. 353-364, Dec. 2017.
- [8] M. Cheah-Mane, L. Sainz, E. Prieto-Araujo, and O. Gomis-Bellmunt, "Impedance-based analysis of harmonic instabilities in HVDC-connected offshore wind power plants," in *International Journal of Electrical Power & Energy Systems*, vol. 106, pp. 420-431, March 2019.
 - [9] W. Xu, "Status and future directions of power system harmonic analysis," in *2003 IEEE Power Engineering Society General Meeting*, Toronto, ON, Canada, vol. 2, pp. 1179-1184, 2003.
 - [10] W. Xu, Z. Huang, Y. Cui, and H. Wang, "Harmonic resonance mode analysis," in *IEEE Transactions on Power Delivery*, vol. 20, no. 2, pp. 1182-1190, April 2005.
 - [11] O. Cartiel, J. J. Mesas, L. Sainz, and A. Fabregas, "A Faster Resonance Mode Analysis Approach Based on a Modified Shifted-Inverse Power Iteration Method," in *IEEE Trans. on Power Delivery*, vol. 38, no. 6, pp. 4145-4156, Dec. 2023.
 - [12] O. Cartiel, J. J. Mesas, and L. Sainz, "Efficient Resonance Mode Analysis-Based Methodology for Resonance Studies in Multi-Terminal Transmission Grids," in *IEEE Transactions on Power Delivery*, vol. 40, no. 1, pp. 287-300, Feb. 2025.
 - [13] L. Sainz, M. Cheah-Mane, L. Monjo, J. Liang, and O. Gomis-Bellmunt, "Positive-Net-Damping Stability Criterion in Grid-Connected VSC Systems," in *IEEE Journal of Emerging and Selected Topics in Power Electronics*, vol. 5, no. 4, pp. 1499-1512, Dec. 2017.
 - [14] J. Pedra, L. Sainz, and Ll. Monjo, "Small Signal Admittance-Based Model of VSCs for Studies of Multi-Terminal HVDC Hybrid AC/DC Transmission Grids," in *IEEE Transactions on Power Systems*, vol. 36, no. 1, pp. 732-743, Jan. 2021.
 - [15] L. Orellana, L. Sainz, E. Prieto-Araujo, and O. Gomis-Bellmunt, "Stability Assessment for Multi-Infeed Grid-Connected VSCs Modeled in the Admittance Matrix Form," in *IEEE Transactions on Circuits and Systems I: Regular Papers*, vol. 68, no. 9, pp. 3758-3771, Sept. 2021.
 - [16] M. Amin and M. Molinas, "Small-Signal Stability Assessment of Power Electronics Based Power Systems: A Discussion of Impedance- and Eigenvalue-Based Methods," in *IEEE Transactions on Industry Applications*, vol. 53, no. 5, pp. 5014-5030, Sept.-Oct. 2017.
 - [17] C. Zhang, M. Molinas, A. Rygg, and X. Cai, "Impedance-Based Analysis of Interconnected Power Electronics Systems: Impedance Network Modeling and Comparative Studies of Stability Criteria," in *IEEE Journal of Emerging and Selected Topics in Power Electronics*, vol. 8, no. 3, pp. 2520-2533, Sept. 2020.
 - [18] L. Orellana, L. Sainz, E. Prieto-Araujo, M. Cheah-Mané, H. Mehrjerdi, and O. Gomis-Bellmunt, "Study of black-box models and participation factors for the Positive-Mode Damping stability criterion," in *International Journal of Electrical Power & Energy Systems*, vol. 148, June 2023.
 - [19] O. Cartiel, L. Sainz, J. J. Mesas and Ll. Monjo, "A Damping Margin Indicator for Compensator Design by the Positive-Mode-Damping Stability Criterion," in *IEEE Transactions on Power Systems* (Early Access).
 - [20] H. Abaali, T. Talbi, R. Skouri, "Comparison of Newton Raphson and Gauss-Seidel methods for power flow analysis," in *International Journal of Energy and Power Engineering*, vol. 12, no. 9, pp. 627 – 633, 2018.
 - [21] "ACTIVSg70k: 70k bus synthetic grid on footprint of eastern United States". Electric Grid Test Case Repository. Accessed: Dec. 14, 2024. [Online]. Available: [ACTIVSg70k Repository](#).